J Membrane Biol (2007) 219:93–104
DOI 10.1007/s00232-007-9065-5

Interactions of Recombinant Mouse Erythrocyte Transglutaminase with Membrane Skeletal Proteins

Edgar Gutierrez · L. Amy Sung

Received: 23 March 2007 / Accepted: 28 June 2007 / Published online: 1 September 2007

Abstract Transglutaminases (TGs) are a family of enzymes that catalyze the formation of covalent γ-glutamyl-ε-lysine crosslinks between glutamine (Q) acyl-donors and lysine (K) acyl-acceptors. Here, we report the cDNA cloning of a TG from mouse reticulocytes, its 4.6-kb message size and high-yield synthesis of recombinant TG in yeast cultures. Its activity was assayed by crosslinking the amine of monodansylcadaverine (DC) onto casein and inside-out vesicles of erythrocytes. The latter contain TG substrates including the anion ion exchanger (AE1) or band 3, and the crosslinking activity was the highest at physiological [GTP] and [ATP] of erythrocytes. To study individually how TG interacts with band 3 and what role P4.2, a pseudo-TG that is normally associated with band 3, may play in their interaction, recombinant cytoplasmic domain of band 3 (cdb3) and P4.2 were also cloned by polymerase chain reaction from mouse reticulocytes, expressed and affinity-purified from *Escherichia coli*. Enzyme-linked immunosorbent assay and Western blot analysis revealed that increasing [$CaCl_2$] enhanced TG-mediated crosslinking of DC to cdb3 but decreased TG binding to cdb3. P4.2 inhibited the TG-mediated crosslinking of cdb3 but stabilized the binding of TG to cdb3 in the presence of calcium. This in vitro study suggests a relationship among TG, cdb3 and P4.2 in erythrocyte membrane during calcium influx.

Keywords γ-Glutamyltransferase · Protein 4.2 · Band 3 · Dansylcadaverine · Crosslinking

E. Gutierrez · L. A. Sung (✉)
Department of Bioengineering and Center for Molecular Genetics, University of California, San Diego, 9500 Gilman Drive, La Jolla, CA 92093-0412, USA
e-mail: amysung@bioeng.ucsd.edu

Introduction

Transglutaminases (TGs) are enzymes that catalyze covalent crosslinks among protein substrates through the formation of intra- or intermolecular γ-glutamyl-ε-lysine bridges (Lorand & Conrad, 1984). In cells or tissues, there are specific protein substrates that serve as glutamine (Q) acyl-donors and others as lysine (K) acyl-acceptors. Under physiological conditions, different TGs are specialized in the crosslinking of particular proteins or tissue structures. For example, coagulation factor XIIIa stabilizes the fibrin clot in hemostasis, prostate TG is involved in semen coagulation in rodents and the hair follicle epidermal-type TG is involved in keratin crosslinking (Lorand & Conrad, 1984; Aeschlimann & Paulsson, 1991).

The mammalian erythrocyte TG is ~80 kDa and was first purified from human whole blood (Lee, Birckbichler & Fesus, 1986). The enzyme is capable of crosslinking erythrocyte membrane skeletal proteins and is activated by a rise in intracellular calcium concentration, $[Ca^{2+}]_i$, above 10 μM (Smith et al., 1981). Specifically, it was shown that Ca^{2+}-loaded erythrocytes in the presence of ^{14}C-histamine covalently labeled this acyl-acceptor to spectrin, band 3, ankyrin, band 4.1 and hemoglobin (Lorand & Conrad, 1984). The calcium activation mechanism is based on large conformational changes after calcium binding, exposing its active site (Bergamini, 1988). TG is also a GTP binding protein with crosslinking activity negatively regulated by the nucleotide (Murthy et al., 1999).

The mouse tissue TG (TGASE) transcript was initially cloned from a mouse macrophage cDNA library (Gentile et al., 1991). The gene was subsequently cloned from a genomic library and named the mouse tissue transglutaminase, *Tgm2* (Nanda et al., 1999). Tissue TG of humans and other mammalian species have been extensively

studied; however, no cDNA has been cloned and characterized directly from reticulocytes. Human TG2 of 77.3 kDa in erythrocytes was identified by proteomic analysis (9% sequence coverage, 3 identified peptides) (Kakhniashvili, Bulla Jr & Goodman, 2004). Here, we report the cloning of a mouse reticulocyte TG cDNA with a complete coding sequence and a 4.6-kb message size in Northern blot analysis (longer than the 3.5-kb transcript of TGASE in mouse macrophages).

Previous attempts at expressing human tissue TG in *Escherichia coli* bacteria yielded poor recoveries of active enzyme and high levels of inclusion bodies (Shi et al., 2002). To better understand the regulation and function of the mammalian erythrocyte TG, in this study we cloned the tissue-specific transcript from mouse reticulocyte cDNA and produced recombinant proteins with enzyme activity in yeast (*Pichia pastoris*). Previously, TG crosslinking activity on membrane skeletal proteins of erythrocytes was assayed by fluorescent labeling of Q acyl-donor substrates remaining in inside-out vesicles (IOVs) with monodansylcadaverine (DC), which serves as an acyl-acceptor. The fluorescence of DC can be directly visualized by ultraviolet illumination, thus allowing for the detection of TG activity and semiquantitative measurements. In this study, we applied this principle and technique to study the activity of recombinant erythrocyte TG in vitro in crosslinking purified recombinant protein substrates and IOVs of erythrocyte membranes. We also explored the regulation of TG activity in IOVs by GTP.

P4.2 is a 72-kDa protein that is a major component of the erythrocyte plasma membrane. It accounts for approximately 5% of the total human erythrocyte membrane protein and binds strongly to the lipid bilayer through *N*-myristoylation (Risinger, Korsgren & Cohen, 1996). P4.2 is normally bound to band 3 and ankyrin (Davis, Lux & Bennett, 1989; Su et al., 2006) in the suspension complex of the membrane skeletal network. Patients deficient in P4.2 developed hemolytic anemia, exhibiting abnormally shaped (spherocytic) and osmotically fragile erythrocytes, suggesting that P4.2 is required to stabilize erythrocyte membrane integrity (Rybicki et al., 1988). In *P4.2*-null mouse models (Peters et al., 1999; Mouro-Chanteloup et al., 2003) it was also shown that P4.2 is important in maintaining normal erythrocyte surface area and normal cation transport.

The cDNA deduced amino acid sequence for human erythrocyte P4.2 is significantly identical to the erythrocyte TG but lacks the critical cysteine residue in the active site required for crosslinking activity (Korsgren et al., 1990; Sung et al., 1990; Rybicki et al., 1994). Due to the significant degree of homology between P4.2 and TG, especially in the putative active site, P4.2 was referred to as a "pseudoenzyme." A band 3 binding site on protein 4.2 was found over a region that is highly conserved within the TG family, specifically the V^{63}RRGQPFTIILYF region on human P4.2, with the $R^{64}R$ motif being essential for binding (Rybicki, Musto & Schwartz, 1995 in addition to residue 200–211 Su et al., 2006). Furthermore, there also exists a region on P4.2 with high homology to the calcium-binding site of TG (Takahashi, Takahashi & Putnam 1986). In this study, to explore a possible functional relationship with TG, P4.2 was cloned from mouse reticulocyte cDNA and the recombinant protein was expressed in *E. coli*.

Band 3 is a 95-kDa Cl/HCO_3 anion exchanger (AE1) in erythrocytes, with several homologs found in the plasma membrane of diverse cell types (Tanner, Martin & High, 1988; Forster et al., 1998). These large molecules span 14 membrane domains in and out of the lipid bilayer and are usually found as dimers or tetramers (Hanspal et al. 1998). They have a functional role of maintaining the acid-base balance by mediating the exchange of chloride and bicarbonate anions across the membrane (Kay & Marchalonis, 1991). In the erythrocyte, band 3 is the most abundant integral membrane protein, with approximately 1.2 million copies per cell, and helps to suspend the membrane skeletal network to the lipid bilayer (Kopito & Lodish, 1985). Band 3, protein 4.2 and ankryin are indeed the major membrane proteins in the suspension complex. Targeted disruption of erythroid band 3 results in spherocytosis and severe hemolytic anemia and dyserythropoiesis in mice (Southgate et al., 1996; Paw et al., 2003).

Band 3 is the most highly available TG substrate on the membrane skeleton (Lorand et al., 1976). Specifically, TG was shown to crosslink Q-30 on band 3 to DC (Murthy et al., 1994). The inherent difficulty in producing or purifying transmembrane proteins with retained function limits the approach to studying the intact band 3 protein. However, nearly half of the protein resides inside the cell, and this soluble cytoplasmic domain of band 3 (cdb3) containing 17 Q and 11 K residues is free to interact with TG and other cytosolic components. In this study, to explore the binding of TG and the crosslinking by TG, cdb3 was cloned from mouse reticulocyte cDNA and the recombinant protein was expressed in *E. coli*.

Despite the remarkable structural similarity between TG and P4.2 and the fact that they both bind to cdb3, the functional relationship between these two homologous proteins remains unclear. The purified recombinant proteins/peptides of cdb3, P4.2 and TG allow for a simplified in vitro system to test their interactions, devoid of complications by the presence of other erythrocyte proteins. The goal is to understand the function of these two homologous proteins in relation to the most abundant and critical ion channel proteins in erythrocytes.

Materials and Methods

Polymerase Chain Reaction Cloning of Mouse Erythrocyte TG

Total RNA from mouse reticulocytes was obtained by injecting C57BL/6J mice (Jackson Laboratory, Bar Harbor, ME) with 0.2 ml of 0.18% phenylhydrazine-HCl, 1 M 4-(2-hydroxyethyl)-1-piperazineethanesulfonic acid (HEPES, pH 7.4) for 5 days (Murthy et al., 1994). Collected blood was washed with and resuspend in 0.15 M NaCl. Erythrocytes were lysed by diluting with four volumes of 0.144 M NH_4Cl (3 mM dithiothreitol [DTT]). Reticulocytes were differentially lysed (over leukocytes) by addition of 1:10 volume of 0.01 M NH_4CO_3 and incubation on ice. Unlysed leukocytes and cellular debris were removed by centrifugation, and nuclear DNA was removed using a sucrose gradient. Total RNA was acid-precipitated by addition of 10% acetic acid to pH 5.1 and centrifuged. Poly A^+ RNA was obtained using an oligo-dT column. Reticulocyte cDNA was produced using a SMART cDNA Sythesis Kit (Clontech, Mountain View, CA). Optimized consensus polymerase chain reaction (PCR) primer sets flanking coding regions of the mouse macrophage transglutaminase (TGASE) (2,083 bp, 686 aa) transcript were designed using MacVector (Accelrys, San Diego, CA). The consensus PCR primers were determined from highly conserved nucleotides among known TG transcripts. AccuPrime-Taq polymerase (Invitrogen, Carlsbad, CA) was used for PCR with the mouse reticulocyte cDNA as the template. PCR products were subcloned using the TOPO-TA cloning kit for DNA sequencing (Invitrogen).

Northern Blot Analysis

Poly A^+ RNA from reticulocytes was separated using standard procedures (Maniatis et al., 1989) on a formaldehyde gel. A 302-bp TG probe was prepared from a TGASE clone (American Type Culture Collection, Manassas, VA) using a sense vector primer and a TGASE sequence antisense primer (5′-TGC CTC TTC ACT GGG ATC TG-3′ position 223 in transcript) according to the manufacturer's protocol for dCTP-^{32}P labeling using the 5′-to-3′ Random Prime Labeling Kit (Amersham Biosciences, Piscataway, NJ). Control macrophage poly A^+ RNA was purified using an oligo-dT column from total RNA obtained from cultured mouse macrophage cell line J774A (American Type Culture Collection).

Expression and Purification of Recombinant TG

The TG coding region was subcloned into the pPICZ yeast vector (Invitrogen). The pPICZ vector contains an in-frame His-tag coding region at the N terminus for affinity purification and an in-frame *myc* tag at the C terminus for detection. Yeast (*P. pastoris*) TG transformants were generated according to methods in the EasySelect *Pichia* Expression Kit (Invitrogen) using the KM71H strain. High-expression yeast clones were grown to high optical density (OD_{600} = 10), and expression was induced with methanol (1%). The induced cell suspension was disrupted using YeastBuster (EMD, San Diego, CA), and the recombinant TG was purified using His-Select HC Nickel Affinity resin (Sigma, St. Louis, MO). Total protein concentration was determined by bicinchoninic acid (BCA) protein assay (Pierce, Rockford, IL)

Casein-DC Crosslinking Assay

Reactions (200 µl) were performed in 96-well microtiter plates containing 200 µg of casein (Sigma), 100 mM Tris-HCl (pH 7.5), 10 mM $CaCl_2$, 10 mM DTT and 4% saturated DC (in 1 M Tris-HCl, pH 7.5) at room temperature. The reaction kinetics at 37°C were recorded for 1 h at 2-min intervals using a GeminiXS SpectraMax fluorometer (Molecular Devices, Sunnyvale, CA) with an excitation wavelength of 330 nm and emission recording at 530 nm.

Preparation of IOVs

Mouse blood (500 µl) was collected from the tail vein using heparin-coated microhematocrit capillary tubes and immediately mixed with one-fifth volume of dextrose citrate-phosphate anticoagulant solution (Sigma). Red blood cells were separated by centrifugation (300 x *g* for 2 min) and washed twice with 10 volumes of a washing buffer (150 mM NaCl, 10 mM KCl, 15 mM Tris-HCl, pH 7.4). The supernatant along with the buffy coat was removed by aspiration after each wash. The erythrocytes were then hypotonically lysed at 4°C in 10 volumes of 5 mM sodium phosphate (pH 7.4), containing phenylmethylsulfonyl fluoride (PMSF), and the membrane pellets were separated by centrifugation (20,000 x *g* for 5 min). The cell membranes were washed in lysis buffer three additional times. The ghost membranes were then passed four times through a 23-gauge needle to allow for IOV formation.

Crosslinking of IOVs by Recombinant TG

Recombinant TG was incubated with 10 µg of IOVs in 100 mM Tris-HCl (pH 7.5, prepared from a 1 M Tris-HCl, DC saturated solution), 10 mM DTT and 10 mM $CaCl_2$ buffer at 37°C for 1 h and analyzed by sodium dodecyl

sulfate-polyacrylamide gel electrophoresis (SDS-PAGE, 10% gel). DC-labeled proteins in the gel were visualized using an SI-1000 UV-Illuminator (Alpha Innotech, San Leandro, CA) capable of frame integration.

PCR Cloning of Mouse Erythrocyte P4.2, Band 3 and cdb3

Optimized PCR primer sets flanking the coding regions of P4.2 (2,092 bp, 691 aa) and band 3 (2,779 bp, 1,227 aa) transcripts were designed using MacVector (Accelrys). AccuPrime-Taq polymerase (Invitrogen) was used for PCR, with the mouse reticulocyte cDNA as the template. PCR products were subcloned using the TOPO-TA cloning kit for DNA sequencing (Invitrogen). The band 3 subcloned plasmid was used to PCR-amplify the cdb3 fragment (1,261 bp, 420 aa), which covers the 5′ end of the translatable region spanning the cytoplasmic domain. An optimized PCR primer pair flanking the N-terminal cdb3 was designed using a hydrophobicity chart generated with MacVector.

Expression and Purification of Recombinant cdb3 and P4.2

BL21-CodonPlus(DE3)-RIL *E. coli* cells (100 μl; Stratagene, La Jolla, CA) were transformed and induced according to the manufacturer's protocol. Aliquots (50 ml) of induced cell suspensions were harvested by centrifugation and stored at −80°C. Cell pellets were resuspended in 8 ml of binding buffer (50 mM $NaPO_4$, 0.5 M NaCl, 10 mM imidazole, pH 7.5). Lysozyme (2 mg) was added to each tube and incubated on ice for 30 min. The solution was sonicated on ice using two 10-s bursts at medium intensity. The lysate was immediately flash-frozen in liquid nitrogen and quickly thawed at 37°C three times. RNase A (10 μg/ml) and DNase I (5 μg/ml) were added and incubated on ice for 15 min. His-tagged proteins were purified by His-Select HC Nickel Affinity (Sigma), and the total protein concentration was determined by BCA protein assay (Pierce). Recombinant proteins were visualized using Invision His-Tag staining (Invitrogen) and by Western blot using an anti-band 3 antibody.

Biotinylation of cdb3

Biotinylation of cdb3 was performed with the EZ-LinkSulfo-NHS-LC-Biotinylation Kit (Pierce). Briefly, 2 mg of cdb3 were diluted in 1 ml of phosphate-buffered saline (PBS) and incubated at room temperature for 30 min with a 20-fold molar excess of Sulfo-NHS-LC-Biotin. The procedure was performed as directed by product protocol to yield approximately three or four amide linkages per cdb3 molecule. The biotinylated protein was then purified from unreacted biotin-hydrazides using a desalting column provided in the kit.

Enzyme-Linked Immunosorbent Assay

Streptavidin coated microtiter plates were prepared with 0.5 μg of streptavidin (Sigma) per well in Tris-buffered saline (TBS: 10 mM Tris–HCl [pH 8.0], 150 mM NaCl) for 2 h at 37°C and washed twice in TBS containing 0.5% v/v Tween (TTBS). Ten micrograms per well of biotinylated cdb3 (1 μg/μl) was then incubated in TBS for an additional 2 h at 37°C and washed twice in TTBS. Nonspecific binding sites were blocked with 1% bovine serum albumin (BSA, fraction V) in TBS for 1 h at 37°C.

TG Binding to cdb3

Enzyme-linked immunosorbent assays (ELISAs) were performed in a total volume of 100 μl. In one experiment, 0.5, 1, 2, 4 or 8 μl of TG (1 μg/μl) were added to each well with a fix concentration of $CaCl_2$ (10 mM) in cdb3 binding buffer (10 mM Tris-HCl [pH 7.5], 10 mM KCl, 1 mM DTT); and the binding was allowed to proceed for 2 h at 37°C. In a second experiment, 4 μg of TG were added to each well in cdb3 binding buffer with increasing concentrations of $CaCl_2$ (0–10 mM) and incubated for 2 h at 37°C. In the third experiment, 2, 4, 8 or 12 μl of P4.2 (1 μg/μl) were added to each well, plus 4 μg of TG, in the presence or absence of 10 mM $CaCl_2$. The wells were then washed twice in TTBS. In each case, a negative control was performed to which no TG or P4.2 was added. An alkaline phosphatase (AP)-conjugated anti-*myc* antibody (Invitrogen) was then used to detect the bound TG. Specifically, a 1:500 dilution of anti-*myc*-AP was incubated in 1% BSA in TBS for 1 h at 37°C and washed three times with TTBS. Binding of the antibody was then measured using the ELISA amplification system (Invitrogen). Absorbance was measured at 490 nm using a SpectraMax 96-well plate spectrophotometer (Molecular Devices).

TG-Mediated DC Crosslinking to cdb3

DC was dissolved to saturation in 1 M Tris-HCl (pH 7.5) at room temperature for 15 min, and the undissolved DC was

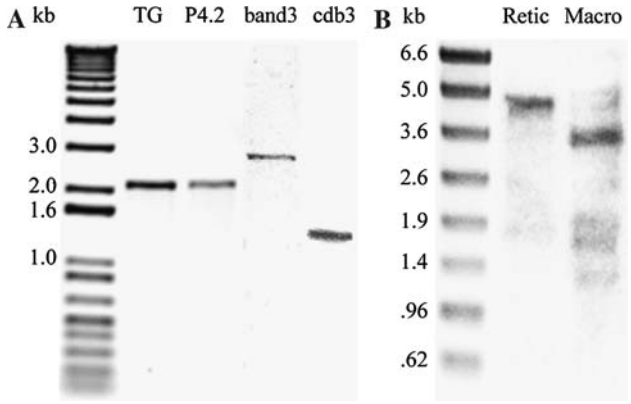

Fig. 1 PCR amplification of TG, P4.2, band 3 and the cdb3 fragment (**a**) from the mouse reticulocyte cDNA and Northern blot analysis (**b**) of TG using mouse reticulocyte and macrophage polyA mRNAs. Results show the mouse TG, P4.2 and band 3 complete coding sequences of 2,083, 2,092 and 2,779 bp, respectively. The 1,261-bp cdb3 sequence was also PCR-amplified from the cDNA. Northern blot of mouse reticulocyte mRNA (*lane 1*) and mouse macrophage mRNA (*lane 2*) probed with the dCTP-^{32}P random primed labeled TGASE fragment. *Lane 1* shows TG mRNA transcript of 4.6 kb. *Lane 2* shows the previously reported mouse macrophage TG mRNA of 3.5 kb

centrifuged out of solution at 20,000 x *g*. The use of DC saturated buffer was a modification of previously used protocols (Lorand et al., 1975). The reaction was performed in 50 µl of 100 mM Tris-HCl with saturated DC (pH 7.5) and 10 mM DTT. In one experiment, 1, 2, 3 or 4 µl of TG (1 µg/µl) in the presence of 10 mM $CaCl_2$ were incubated with 4 µl of cdb3 (1 µg/µl) at 37°C for 1 h. In a second experiment, 2 µg of TG was incubated with 4 µg of cdb3 and with increasing $CaCl_2$ concentration (0–10 mM) at 37°C for 1 h. In a third experiment, 0.5, 1.0, 2.5 or 5 µl of P4.2 (1 µg/µl) were incubated in the presence of 4 µg of TG and 4 µg of cdb3 with 10 mM $CaCl_2$ at 37°C for 1 h. In each case, a negative control was performed to which no TG or P4.2 was added. The samples were analyzed by SDS-PAGE, and the proteins crosslinked by DC were visualized with an ultraviolet (UV) illuminator (Alpha-Innotech).

Western Blot Analysis

Cell lysates, ghost membranes or recombinant proteins were solubilized in Laemmli sample buffer containing 0.1 M DTT and separated by SDS-PAGE (10% gel). Proteins were transblotted onto nitrocellulose filters and stained with Ponceau S, and filters were blocked in TTBS containing 1% BSA for at least 1 h. To detect TG, a horseradish peroxidase (HRP)-conjugated anti-*myc* antibody (Invitrogen) was used at a 1:2,000 dilution in blocking buffer for 1 h and washed three times in TTBS. To detect cdb3, a polyclonal anti-band 3 antibody (a gift from Dr. Luanne Peters, Jackson Laboratory) was used at a 1:2,000 dilution followed by HRP-conjugated secondary antibody. Signals were visualized using an enhanced chemiluminescence (ECL) detection system (Amersham, Arlington Heights, IL).

Results

PCR Cloning of Mouse Erythrocyte TG

Using mouse reticulocyte cDNA as the template, oligo primer pair for TG yielded a PCR product of 2,083 bp (Fig. 1a). The PCR products were subcloned, and positive clones which encode the entire 686 residues were verified by nucleotide sequencing.

Northern Blot Analysis

Northern blot analysis, using a PCR fragment containing a 5′ end mouse macrophage TG coding sequence (302 bp) as the probe, revealed a single band of 4.6 kb (lane 1) in the reticulocyte poly A^+ mRNA (Fig. 1b). Concurrently, a 3.5-kb band (lane 2) was found in the mouse macrophage mRNA.

Expression and Purification of Recombinant TG

TG cloned from reticulocytes was expressed in KM71H *P. pastoris* cells and purified using a Ni column (Fig. 2a). Western blot analysis using anti-*myc* antibodies of the transformed yeast lysate and the affinity-purified TG confirmed the in-frame expression and the expected size of ~80 kDa (Fig. 2b). TG was expressed in high-density yeast cultures (OD_{600} = 10) at 20 mg/liter culture. Purification was done under native conditions to ensure enzyme activity, even though purification under native conditions significantly reduced the yield compared to denaturing conditions. Using a nickel affinity column, greater than 90% of the bound recombinant protein was collected within the first three 0.5-ml fractions when eluted with 200 mM imidazole. A doublet was detected by Coomassie blue staining and Western blot analysis. It is likely that they represent the two states of the enzyme, based on the finding that GTP binding of TG produces a shift in the anodic mobility during electrophoresis. It has been reported that in the absence of nucleotides TG is observed as two bands running closely together: a slow (unbound state) and a fast (bound state) (Murthy et al., 1999).

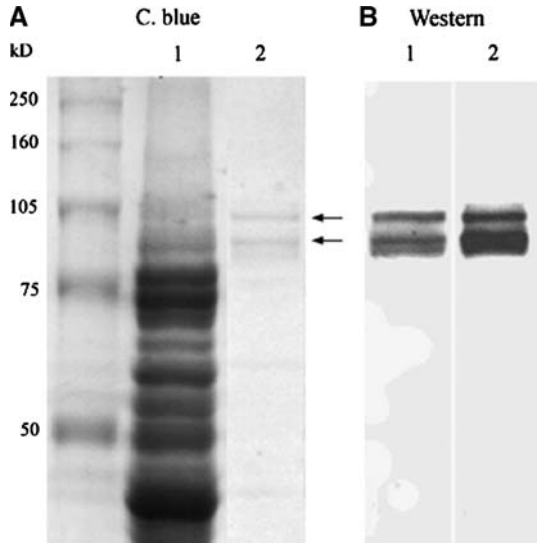

Fig. 2 Expression and purification of recombinant mouse erythrocyte TG. **a** Coomassie blue staining of yeast lysate expressing TG (*lane 1*) and Ni column purified fraction (*lane 2*). The calculated molecular mass of TG is ~80 kDa. **b** Western blot analysis of the same gel using anti-*myc* antibodies confirms the correct reading frame. *Double arrows* point to the purified TG which runs as a doublet

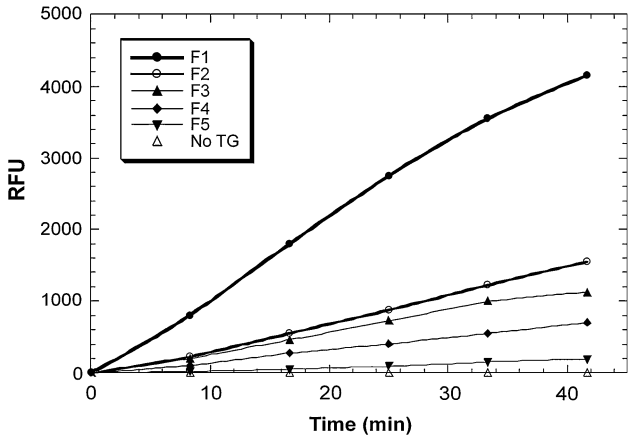

Fig. 3 Kinetic assay showing the incorporation of fluorescent DC to long casein molecules catalyzed by recombinant TG. The plot shows the relative enzymatic activity of various column fractions (F1-F5) measured in relative fluorescent units (*RFUs*)

Enzymatic Activity of Recombinant TG

The relative activities of TG in each of the eluted fractions were determined by measuring the rate of DC incorporation into casein, a known substrate for TG (Fig. 3). The first eluted fraction (F1) had the highest concentration of enzyme (determined by BCA protein assay) and was the most active fraction. Recombinant TG for F1 had a calculated purification factor of 128-fold. The kinetic analysis resulted in a specific activity for TG (in crosslinking DC to casein) of approximately 820 relative fluorescent units/(mg · min) or 670 pmol DC/(mg · min). The enzyme kinetics plot revealed first-order incorporation of DC at high concentration, as expected.

Crosslinking of IOVs by Recombinant TG

To study the crosslinking activity of TG on erythrocyte membrane skeletal proteins, a total protein profile of the erythrocyte ghost membrane was analyzed by SDS-PAGE (10% gel) as a reference (Fig. 4a). Incubation of IOV with DC and recombinant TG produced intensely labeled band 3, and spectrin/ankryin (Fig. 4b). There was also moderate crosslinking in the region of band 4.1. Saturation of the crosslinking was achieved with approximately 4 μg of TG during 1-h incubation (Fig. 4b). TG crosslinking activity with IOVs could only be visualized with samples that contained calcium concentrations higher than 1 mM. No activation was observed for calcium concentrations lower than 0.1 mM (Fig. 4c). The intensity of crosslinking increased with increasing calcium up to 10 mM. Aside from intensity, the crosslinking profiles were the same for all calcium concentrations with detectable TG activity.

Regulation of TG Activity by Nucleotides

Incubations of IOVs with DC and recombinant TG with increasing [GTP] (at a fixed 10 mM concentration of $CaCl_2$) showed inhibition of TG activity when [GTP] > 0.05 mM, with optimal activation between 0.01 and 0.05 mM (Fig. 5a). Incubations with increasing [ATP] were also conducted since no regulation of TG by ATP has been reported. [ATP] showed optimal activation of TG between 0.5 and 2 mM (Fig. 5b) (at [$CaCl_2$)] = 10 mM). ATP (5 mM) significantly inhibited TG activity, and only minimal activity was observed at 10 mM ATP (Fig. 5b).

PCR Cloning of Mouse Erythrocyte P4.2, Band 3 and cdb3

To study the interaction among TG, band 3 and P4.2, recombinant proteins or peptides were made. Using mouse reticulocyte cDNA as templates, oligo primer sets for P4.2, band 3 and cdb3 yielded PCR products encoding the entire reading frames of 2,092, 2,779 and 1,261 bp, respectively (Fig. 1a). The PCR products encoded 691, 911 and 412 residues of P4.2, band 3 and cdb3, respectively. The PCR products were subcloned, and positive clones were verified by nucleotide sequencing.

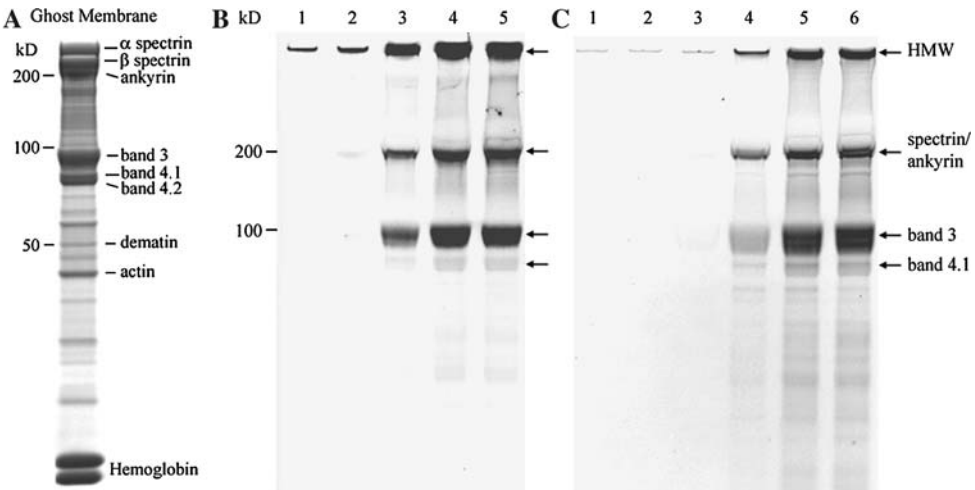

Fig. 4 Protein profile of erythrocyte ghost membrane by SDS-PAGE/Coomassie blue staining (**a**) and DC labeling (crosslinking) of IOVs with recombinant TG at fixed 10 mM [$CaCl_2$] (**b**) and at increasing [$CaCl_2$] (**c**). All lanes have 10 μg IOVs. **b** *Lane 1*, no DC (well is illuminated due to UV scatter). *Lanes 2-5* contain 0, 2, 4 and 6 μg TG, respectively. *Lane 2* shows weak endogenous TG crosslinking activity. **c** All lanes contained 4 μg of TG. *Lanes 1-6* contain 0.025, 0.05, 0.1, 1, 5 and 10 mM $CaCl_2$, respectively

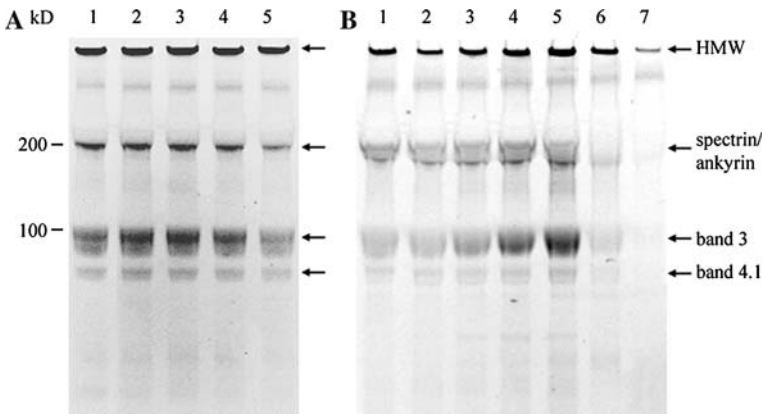

Fig. 5 SDS-PAGE analysis of DC crosslinking of IOVs by recombinant TG with increasing amounts of GTP (**a**) and increasing amounts of ATP (**b**) at a fixed 10 mM [$CaCl_2$]. All lanes have 10 μg IOVs and 4 μg TG. **a** *Lanes 1-5* contain 0, 0.01, 0.05, 0.1 and 0.5 mM GTP, respectively. **b** *Lanes 1-7* contain 0, 0.1, 0.25, 0.5, 2, 5 and 10 mM ATP, respectively

Expression and Purification of Recombinant cdb3 and P4.2

To express recombinant P4.2 and cdb3, corresponding sequences were subcloned into the TOPO-pET100 bacterial expression vector. The pET100 vector contains an in-frame His-tag coding region at the N terminus for affinity purification. Both cdb3 and P4.2 were expressed in *E. coli* cells (Fig. 6). cdb3 (~50 kDa, residues 1-412) was expressed to greater than 20% of total bacterial proteins (Fig. 6a). P4.2 (~75 kDa, 691 residues) was expressed to a lesser extent (Fig. 6d). Both proteins were detectable within 1 h of induction (data on 3 and 5 h are shown). Soluble cdb3 and P4.2 were expressed in *E. coli* at 9.5 and 2.1 mg/liter culture, respectively, as determined by BCA protein assay. Both recombinant proteins expressed in *E. coli* showed evidence of significant inclusion body formation in the insoluble fraction (Fig. 6f, g). Invision His-tag fluorescence of both proteins confirmed the in-frame expression and correct size (Fig. 6b, e). There was no noticeable intracellular degradation of cdb3 as observed by Invision His-tag fluorescence (Fig. 6b), but a small degree was detected by a more sensitive Western blot (Fig. 6c).

TG Binding to cdb3 Analyzed by ELISA

Before TG-mediated crosslinking was analyzed , the binding of TG to cdb3 was tested by ELISA, where TG was detected by anti-myc antibodies conjugated with AP. The signals for TG bound to cdb3 increased linearly with increasing amounts of TG in solution, as expected (Fig. 7a), both in the presence and in the absence of $CaCl_2$. The binding was sensitive to [$CaCl_2$]. At a saturating level of calcium (10 mM), signals for TG bound to cdb3 were reduced by more than 50% of that in the absence of calcium (Fig. 7a).

Effect of Ca^{2+} on TG Binding to cdb3

A more detailed analysis was carried out to include near-membrane microdomain concentrations of [$CaCl_2$] ranging 0.25–0.5 mM. At submillimolar concentrations of [$CaCl_2$] (0.25–1.0 mM), TG binding to cdb3 was reduced to ~75% of the level in the absence of calcium (Fig. 7b). At millimolar concentrations of [$CaCl_2$] (2.5–10 mM), TG binding to cdb3 decreased further, reaching a minimal level at ~30% of that in the absence of calcium.

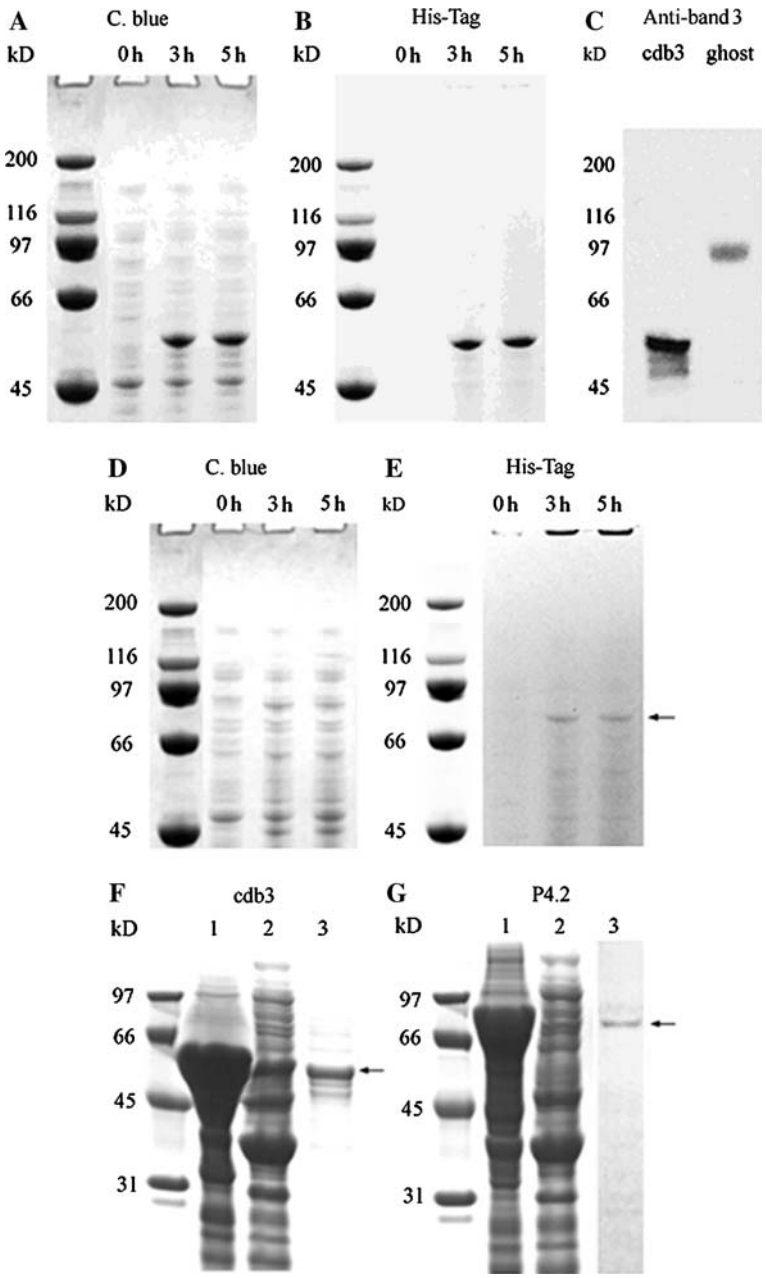

Fig. 6 Expression and purification of cdb3 and P4.2. **a** Total proteins of a cdb3 BL21/pET100 (*E. coli*) clone 0, 3 and 5 h after isopropyl β-D-1-thiogalactopyranoside (IPTG) induction, separated by SDS-PAGE and stained by Coomassie blue. **b** Invision His-tag fluorescence confirmed the in-frame expression of cdb3 and correct size of the recombinant protein (~50 kDa). **c** Western blot analysis of Ni column purified recombinant cdb3 and mouse erythrocyte ghost membrane, where the full-length native band 3 (~95 kDa) was also recognized. **d** Total proteins of a P4.2 BL21/pET100 (*E. coli*) clone at 0, 3 and 5 h after IPTG induction, separated by SDS-PAGE and stained by Coomassie blue. **e** Invision His-tag fluorescence. *Arrow* points to recombinant P4.2 (~75 kDa). **f, g** Inclusion bodies and purified soluble recombinant proteins: **f** cdb3, **g** P4.2. *Lane 1*, insoluble fraction; *lane 2*, soluble fraction; and *lane 3*, purified recombinant proteins (indicated by *arrows*). All were derived from BL21/pET100 (*E. coli*) corresponding transformants, separated by SDS-PAGE and stained by Coomassie blue

TG-Mediated DC Crosslinking to cdb3

The crosslinking of DC to cdb3 catalyzed by TG could be visualized by SDS-PAGE. After incubation of the reaction mixture containing DC, cdb3 and TG for 1 h, samples were subjected to SDS-PAGE and the fluorescence signals of DC on cdb3 could be visualized when the gel was exposed under UV. Figure 8a shows the increased DC signals crosslinked to cdb3 (~50 kDa, arrowed) with increasing amounts of TG. Figure 8b shows the increasing fluorescence DC signals crosslinked to cdb3 with increasing [$CaCl_2$]. This two-protein component assay allowed us to directly visualize and quantify a significant increase in TG crosslinking on cdb3 with increasing calcium.

Effects of P4.2 on TG Binding and Crosslinking cdb3

The effect of P4.2 in the TG-mediated DC crosslinking to cdb3 was analyzed in vitro by incubating the three recombinant proteins in the absence of other potentially interacting proteins in whole-cell assays. Western blot analysis (Fig. 9a) showed that monomeric cdb3 crosslinking into high-molecular weight complex was inhibited by increasing amounts of P4.2. UV analysis (Fig. 9b) showed that total TG-mediated DC labeling or crosslinking on all substrates was inhibited by P4.2.

To see whether P4.2 inhibition of TG-mediated crosslinking was due to the inhibition of TG binding to cdb3, we conducted an ELISA (Fig. 9c). The result showed that in

the absence of Ca^{2+} P4.2 did not inhibit the binding of TG to cdb3. In the presence of saturating 10 mM $CaCl_2$, P4.2 significantly inhibited the dissociation of TG from cdb3. Without P4.2, TG remaining bound to cdb3 was decreased by more than sixfold.

Discussion

Cloning of mouse erythrocyte TG from reticulocyte mRNA settled the question as to what type of TG exists in erythrocytes. Except for some minor mismatches (probably sequencing errors), the cDNA is that of the mouse tissue transglutaminase (Tgm2). Northern blot analysis detected the Tgm2 transcript of published size (3.5 kb) in the mouse macrophage mRNA (Fig. 1b). Northern analysis, however, revealed a larger 4.6-kb TG transcript in the reticulocyte mRNA (Fig. 1b). The difference in size indicates the existence of distinct transcripts generated from the same tissue TG gene that are made differently by some mechanisms, perhaps by different transcriptional start sites. The lack of detectable macrophage TG mRNA in the reticulocyte mRNA confirmed the reticulocyte preparation was devoid of contaminating RNA from white blood cells.

It is generally believed that TG is a soluble protein in the cytoplasm. A high level of TG activity, however, has also been found in the purified erythrocyte membrane fraction (Magnani et al., 1980; Signorini et al., 1988; Brenner & Wold, 1978). Yet, it is unclear whether TG is bound to band 3 and whether there is a relationship between its binding and enzymatic crosslinking activity. Given that band 3 is a Q acyl-donor for TG and a cdb3 binding site on P4.2 is conserved in TG, it is likely that TG may be associated with band 3. In this study, we indeed demonstrated specific binding of TG to cdb3 by ELISA (Fig. 7a). We further show that increasing [$CaCl_2$] lowered TG binding to cdb3 while increasing TG-mediated crosslinking of DC (Figs. 7, 8). The reciprocal relationship between the cdb3 binding of TG and crosslinking by TG with regard to calcium implicates that binding and crosslinking may occur as two separate steps or events. It also suggests that the conformational change triggered by calcium and needed for the crosslinking may also facilitate the dissociation of TG from cdb3. Thus, we may envision that some TG may be associated with cdb3 on the membrane before the calcium influx and after the catalytic event in response to the surge of calcium concentration near the membrane fall off cdb3 (Heidelberger et al., 1994; Wu, Tucker & Fettiplace, 1996). When $[Ca2^+]_i$ returns to normal, due to the action of calcium pumps, some cytosolic TG may again bind to cdb3 and become membrane-bound. Cycles may go on until all Q acyl-donors are crosslinked and/or cells are sequestered due to changes in membrane properties induced by TG crosslinking.

The sequence homology between TG and P4.2 has raised an interesting question as to why a pair of true enzyme and pseudoenzyme coexists in erythrocytes and

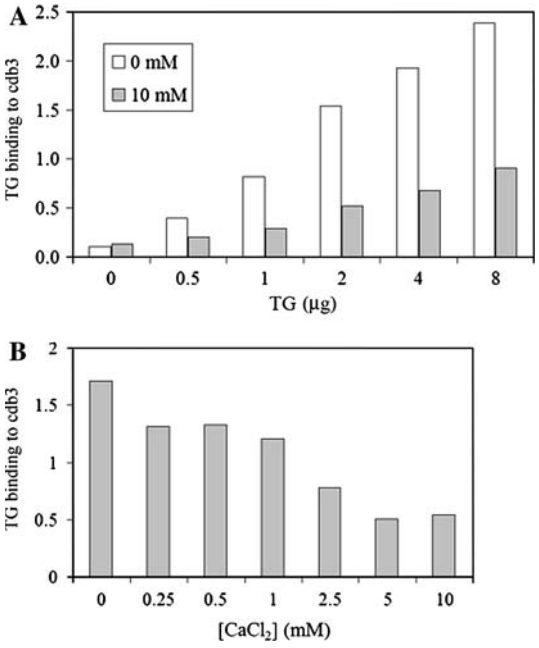

Fig. 7 The effects of calcium on TG binding to cdb3 using ELISA. **a** Binding of TG to cdb3 in the absence of calcium and in the presence of 10 mM calcium (n = 2). **b** Binding of TG to cdb3 with increasing concentration of calcium (n = 2)

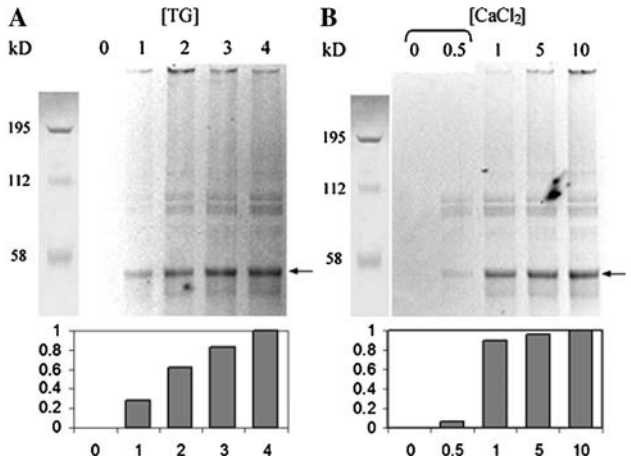

Fig. 8 TG-mediated DC crosslinking to cdb3 analyzed by SDS-PAGE. **a** TG (0, 1, 2, 3 or 4 μg) was used (indicated above each lane) in reaction with a saturation level of 10 mM $CaCl_2$. *Arrows* indicate the position of cdb3 (~50 kDa). DC fluorescence was visualized under UV light. **b** TG (2 μg) was used in the DC crosslinking reaction at the [$CaCl_2$] (mM) indicated above each lane. Signals at the top of the gels may represent cdb3 oligomers crosslinked by TG. Bracket indicates the range of near membrane calcium concentrations. *Panels at the bottom* show signals of DC at monomeric cdb3 relative to the strongest signals

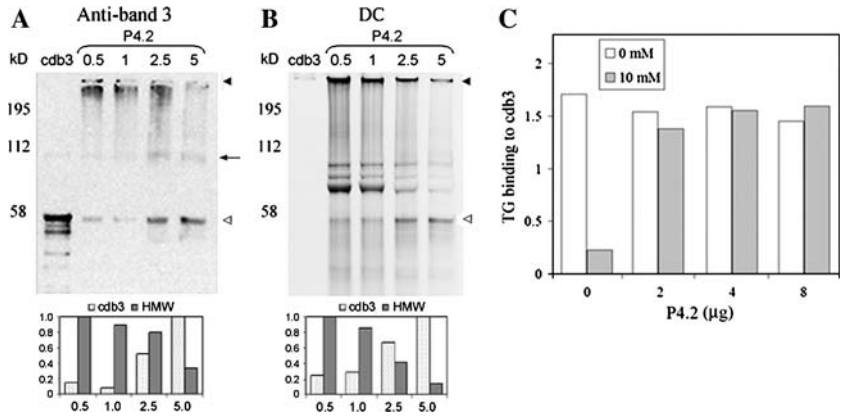

Fig. 9 P4.2 inhibition of TG-mediated crosslinking of cdb3 and influence on TG binding to cdb3. **a** Western blot analysis using anti-band 3 antibodies. Decreased amounts of high-molecular weight polymers are clear with increasing P4.2. *Arrow* points to a possible cdb3 doublet. *Panel below each figure* shows relative degree of cdb3 crosslinking and of high-molecular weight polymers formed based on the DC signals. **b** DC signals detected by UV light on a gel after SDS-PAGE. *Lane 1* is cdb3 (10 μg). *Lanes 2-5* are reactions with 4 μg of cdb3, 5 μg of TG and 0.5, 1.0, 2.5 and 5 μg of P4.2, respectively, in the presence of 10 mM $CaCl_2$. *Open arrowhead* points to cdb3 (50 kDa); *closed arrowhead* points to high molecular weight (*HMW*) polymers. The three bands between the monomeric cdb3 and the high molecular weight complex are likely to be the TG doublet and P4.2 based on the molecular weight. **c** TG binding to cdb3 in the presence of P4.2. Detection was performed by ELISA using an antibody against the *myc* tag in TG with cdb3 attached to the wells ($n = 2$). In the absence of $CaCl_2$, P4.2 did not alter the binding of TG to cdb3. In the presence of 10 mM $CaCl_2$, P4.2 prevented the dissociation of TG from cdb3

what their functions may be. While the enzymatic activity of TG offers a valuable clue, the lack of enzymatic activity in the much more abundant P4.2 adds to the mystery. Thus far, P4.2 has only been shown to have structural functions, as a major component in the suspension complex of the erythrocyte membrane skeleton, and may regulate the cation transport function of band 3. Here, we uncovered interesting functional relationships between erythrocyte TG and P4.2, especially regarding their interaction with cdb3, and have set the groundwork for future work.

The effects of P4.2 in the TG-mediated DC crosslinking of cdb3 and binding of TG to cdb3 were not parallel. P4.2 prevented cdb3 from being crosslinked into high-molecular weight polymers (Fig. 9a), suggesting that the Q acyl-donor site on cdb3 may be blocked by bound P4.2 and/or that the conformational change of TG needed for crosslinking and triggered by calcium may be prevented by P4.2. On the contrary, binding of TG to cdb3 was not inhibited by P4.2. Instead, P4.2 stabilized the binding of TG. Without P4.2, TG would catalyze the crosslinking and detach from cdb3 in the presence of calcium (Fig. 9c). Understanding the mechanism by which P4.2 stabilized TG binding to cdb3 and prevented it from crosslinking cdb3 deserves more study.

The finding that only at elevated [Ca^{2+}] does P4.2 have an effect on TG (not in the absence of Ca^{2+}) is interesting. This suggests that both TG and P4.2 can bind to cdb3 under normal physiological conditions. Only when there is a Ca^{2+} influx, which activates TG, does P4.2 begin to interfere with TG. Whether P4.2 itself, which has a potential Ca^{2+} binding site, also undergoes transformation in response to Ca^{2+} is an interesting question. Without P4.2 to inhibit the TG crosslinking activity, cdb3 would tend to form more crosslinks. This may explain why P4.2-deficient erythrocytes may be prematurely sequestered, leading to their shorter life spans and to hemolytic anemia (Peters et al., 1999; Mouro-Chanteloup et al., 2003). cdb3 dimer was not DC-crosslinked (Fig. 9a, b), suggesting that the sites for TG crosslinking may be blocked once they are dimerized.

Stabilizing TG binding to cdb3 and preventing its crosslinking activity by P4.2 during transient calcium influx in circulating erythrocytes may be part of the mechanism by which P4.2 regulates the mechanical properties of normal erythrocytes. It is known that erythrocyte membrane rigidity increases as cells age in vivo, together with an increase in high-molecular weight crosslinked polymers (Lorand et al., 1976). Aside from oxidative damage, the erythrocyte membrane stiffness may also be increased by covalent protein crosslinks mediated by intracellular TG. This in vitro system of recombinant proteins not only proved to be a useful tool in analyzing how these major proteins in the suspension complex interact but may help elucidate the potential functional roles of a pair of homologous proteins, P4.2 and TG, in their specific interactions with the cytoplasmic domain of band 3, the important Cl/HCO_3 anion transporter and one of the most abundant erythrocyte transmembrane proteins.

We confirmed that TG is activated by [$CaCl_2$] $>$ 0.5 mM and inhibited by [GTP] $>$ 0.05 mM (Figs. 4c, 5a).

Surprisingly, ATP showed inhibition of TG at >5 mM (Fig. 5b). Therefore, TG appears to have optimal activation within the physiological range of [GTP] and [ATP] (Fig. 5) and is ready for crosslinking activity upon calcium influx.

Acknowledgement These experiments were conducted either in the Molecular Bioengineering Laboratory or in the Biotech Core of the Bioengineering Department, initially established with support by the Whitaker Foundation. We thank Dr. Laszlo Lorand for helpful information in cloning of mouse erythrocyte TG. We thank Dr. Luann Peters at the Jackson Laboratory for providing antibodies against band 3.

References

Aeschlimann D, Paulsson M (1991) Crosslinking of laminin-nidogen complexes by tissue transglutaminase. A novel mechanism for basement membrane stabilization. J Biol Chem 266:15308–15317

Bergamini CM (1988) GTP modulates calcium binding and cation-induced conformational changes in erythrocyte transglutaminase. FEBS Lett 239:255–258

Brenner SC, Wold F (1978) Human erythrocyte transglutaminase. Purification and properties. Biochim Biophys Acta 522:74–83

Davis L, Lux SE, Bennett V (1989) Mapping the ankyrin-binding site of the human erythrocyte anion exchanger. J Biol Chem 264:9665–9672

Forster RE, Gros G, Lin L, Ono Y, Wunder M (1998) The effect of 4,4'-diisothiocyanato-stilbene-2,2'-disulfonate on CO_2 permeability of the red blood cell membrane. Proc Natl Acad Sci USA 95:15815–15820

Gentile V, Saydak M, Chiocca EA, Akande O, Birckbichler PJ, Lee KN, Stein JP, Davies PJ (1991) Isolation and characterization of cDNA clones to mouse macrophage and human endothelial cell tissue transglutaminases. J Biol Chem 266:478–483

Hanspal M, Golan DE, Smockova Y, Yi SJ, Cho MR, Liu S-C, Palek J (1998) Temporal synthesis of band 3 oligomers during terminal maturation of mouse erythroblasts. Dimers and tetramers exist in the membrane as preformed stable species. Blood 92:329–338

Heidelberger R, Heinemann C, Neher E, Matthews G (1994) Calcium dependence of the rate of exocytosis in a synaptic terminal. Nature 371:513–515

Kahniashvili DG, Bulla Jr LA, Goodman SR (2004) The human erythrocyte proteome. Analysis by ion trap mass spectrometry. Mol Cell Proteomics 3:501–509

Kay MM, Marchalonis JJ (1991) Molecular mapping of the active site of an aging antigen. Adv Exp Med Biol 307:303–316

Kopito RR, Lodish HF (1985) Primary structure and transmembrane orientation of the murine anion exchange protein. Nature 316:234–238

Korsgren C, Lawler J, Lambert S, Speicher D, Cohen CM (1990) Complete amino acid sequence and homologies of human erythrocyte membrane protein band 4.2. Proc Natl Acad Sci USA 87:613–617

Lee KN, Birckbichler PJ, Fesus L (1986) Purification of human erythrocyte transglutaminase by immunoaffinity chromatography. Prep Biochem 16:321–335

Lorand L, Conrad SM (1984) Transglutaminases. Mol Cell Biochem 58:9–35

Lorand L, Shishido R, Parameswaran KN, Steck TL (1975) Modification of human erythrocyte ghosts with transglutaminase. Biochem Biophys Res Commun 67:1158–1166

Lorand L, Weissmann LB, Epel DL, Bruner-Lorand J (1976) Role of the intrinsic transglutaminase in the Ca^{2+}-mediated crosslinking of erythrocyte proteins. Proc Natl Acad Sci USA 73:4479–4481

Magnani M, Cucchiarini L, Stocchi V, Bossu M, Dacha M (1980) Erythrocytes of different ages: a new method of "in vivo" preparation. Biochem Exp Biol 16:13–18

Mouro-Chanteloup I, Delaunay J, Gane P, Nicolas V, Johansen M, Brown EJ, Peters LL, Van Kim CL, Cartron JP, Colin Y (2003) Evidence that the red cell skeleton protein 4.2 interacts with the Rh membrane complex member CD47. Blood 101:338–344

Murthy SN, Lomasney JW, Mak EC, Lorand L (1999) Interactions of G(h)/transglutaminase with phospholipase Cdelta1 and with GTP. Proc Natl Acad Sci USA 96:11815–11819

Murthy SN, Wilson J, Zhang Y, Lorand L (1994) Residue Gln-30 of human erythrocyte anion transporter is a prime site for reaction with intrinsic transglutaminase. J Biol Chem 269:22907–22911

Nanda N, Iismaa SE, Copeland NG, Gilbert DJ, Jenkins N, Graham RM, Sutrave P (1999) Organization and chromosomal mapping of mouse Gh/tissue transglutaminase gene (Tgm2). Arch Biochem Biophys 366:151–156

Paw BH, Davidson AJ, Zhou Y, Li R, Pratt SJ, Lee C, Trede NS, Brownlie A, Donovan A, Liao EC, Ziai JM, Drejer AH, Guo W, Kim CH, Gwynn B, Peters LL, Chernova MN, Alper SL, Zapata A, Wickramasinghe SN, Lee MJ, Lux SE, Fritz A, Postlethwait JH, Zon LI (2003) Cell-specific mitotic defect and dyserythropoiesis associated with erythroid band 3 deficiency. Nat Genet 34:59–64

Peters LL, Jindel HK, Gwynn B, Korsgren C, John KM, Lux SE, Mohandas N, Cohen CM, Cho MR, Golan DE, Brugnara C (1999) Mild spherocytosis and altered red cell ion transport in protein 4. 2-null mice. J Clin Invest 103:1527–1537

Risinger MA, Korsgren C, Cohen CM (1996) Role of *N*-myristylation in targeting of band 4.2 (pallidin) in nonerythroid cells. Exp Cell Res 229:421–431

Rybicki AC, Heath R, Wolf JL, Lubin B, Schwartz RS (1988) Deficiency of protein 4.2 in erythrocytes from a patient with a Coombs negative hemolytic anemia. Evidence for a role of protein 4.2 in stabilizing ankyrin on the membrane. J Clin Invest 81:893–901

Rybicki AC, Schwartz RS, Qiu JJ, Gilman JG (1994) Molecular cloning of mouse erythrocyte protein 4.2: a membrane protein with strong homology with the transglutaminase supergene family. Mamm Genome 5:438–445

Rybicki AC, Musto S, Schwartz RS (1995) Identification of a band-3 binding site near the N-terminus of erythrocyte membrane protein 4.2. Biochem J 309(pt 2):677–681

Shi Q, Kim SY, Blass JP, Cooper AJ (2002) Expression in Escherichia coli and purification of hexahistidine-tagged human tissue transglutaminase. Protein Expr Purif 24:366–373

Signorini M, Bortolotti F, Poltronieri L, Bergamini CM (1988) Human erythrocyte transglutaminase: purification and preliminary characterisation. Biol Chem Hoppe Seyler 369:275–281

Smith BD, La Celle PL, Siefring GE Jr, Lowe-Krentz L, Lorand L (1981) Effects of the calcium-mediated enzymatic crosslinking of membrane proteins on cellular deformability. J Membr Biol 61:75–80

Southgate CD, Chishti AH, Mitchell B, Yi SJ, Palek J (1996) Targeted disruption of the murine erythroid band 3 gene results in spherocytosis and severe haemolytic anaemia despite a normal membrane skeleton. Nat Genet 14:227–230

Su Y, Ding Y, Jiang M, Jiang W, Hu X, Zhang Z (2006) Associations of protein 4.2 with band 3 and ankyrin. Mol Cell Biochem 289:159–166

Sung LA, Chien S, Chang LS, Lambert K, Bliss SA, Bouhassira EE, Nagel RL, Schwartz RS, Rybicki AC (1990) Molecular cloning

of human protein 4.2: a major component of the erythrocyte membrane. Proc Natl Acad Sci USA 87:955–959

Takahashi N, Takahashi Y, Putnam FW (1986) Primary structure of blood coagulation factor XIIIa (fibrinoligase, transglutaminase) from human placenta. Proc Natl Acad Sci 83:8019–8023

Tanner MJ, Martin PG, High S (1988) The complete amino acid sequence of the human erythrocyte membrane anion-transport protein deduced from the cDNA sequence. Biochem J 256:703–712

Wu YC, Tucker T, Fettiplace R (1996) A theoretical study of calcium microdomains in turtle hair cells. Biophys J 71:2256–2275